

An Analysis of Ultrasonically Rotating Droplet with Moving Particle Semi-implicit and Distributed Point Source Method in a Rotational Coordinate

回転座標系下の粒子法と分布点音源法による超音波浮揚液滴回転解析

Yuji WADA^{1†}, Kohei YUGE¹, Hiroki TANAKA² and Kentaro NAKAMURA²
(¹Fac. Sci. & Tech., Seikei Univ.; ²FIRST, Tokyo Tech.)

和田有司^{1†}, 弓削康平¹, 田中宏樹², 中村健太郎² (¹成蹊大 理工, ²東工大 FIRST)

1. Introduction

Ultrasonic levitation has recently been drawing attention as a way of non-contact transportation of small objects, such as liquid droplets, in bioengineering and manufacturing industry. The small objects in the finite amplitude sound field have been known to be trapped near the pressure node of the standing wave with the effect of acoustic radiation force [1-2]. Many experimental reports [3] are presented related to the droplet levitation and their shape and streaming field on the droplet. The droplet with large volume is reported to rotate along its spheroidal axis when they are exposed in the intense sound pressure field. Biswas, et. al [4] experimentally discussed the droplet rotation using an ultrasonic vibrator and a pair of acoustic driver, which works as an levitator and an artificial visco-acoustic generator, respectively. Authors [5,6] have proposed a coupled analysis method using distributed point source method (DPSM, [7]) and moving particle semi-implicit (MPS, [8]) method to simulate the rotation of the ultrasonically levitated droplet. The droplet rotation in the initial stage has been successfully calculated, however, the calculation routine is unstable or inaccurate in the latter stage calculation.

In this paper, the amendment of the calculation routine using least square MPS (LS-MPS, [9]) and the rotational coordinate is suggested.

2. Calculation Procedure

Acoustic radiation force considering visco-acoustic torque working on volume dV are expressed by the sound pressure p and particle velocity \mathbf{u} , with dS , n , ρ_0 , c , ω , and ν are the boundary surface, surface normal, density, sound speed, angular frequency, and dynamic viscosity as

$$\mathbf{F}dV = (-P_{rad}\mathbf{n} + \boldsymbol{\tau}_R)dS, \quad (1)$$

$$P_{rad} = \langle p^2 \rangle / (2\rho_0 c^2) + (\rho_0 / 2) \langle \mathbf{u}^2 \rangle,$$

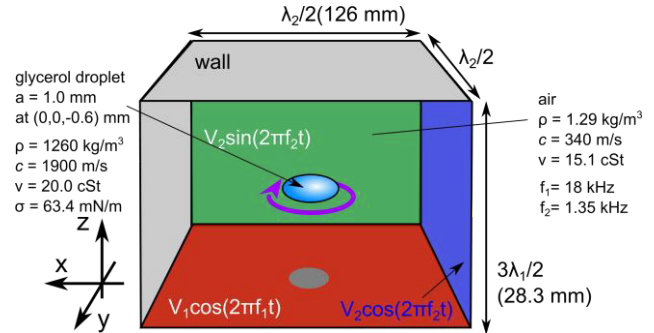


Fig. 1 Problem geometry for the ultrasonic droplet levitation

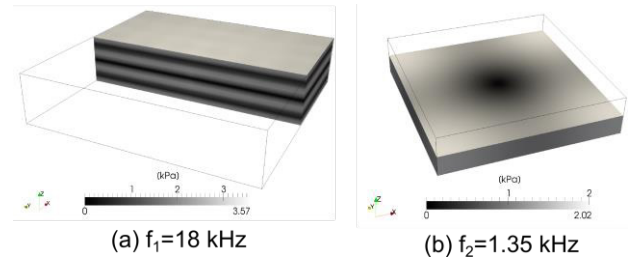


Fig. 2 Sound pressure distribution from (a) ultrasonic levitator and (b) acoustic driver.

$$\boldsymbol{\tau}_R = -\rho_0 \langle v_b \mathbf{u} \rangle,$$

$$v_b = \sqrt{j\omega\nu} \left(\frac{p}{\rho_0 c^2} - \frac{1}{j\omega} \frac{\partial u_n}{\partial n} \right). \quad (2)$$

The sound pressure and particle velocity are calculated using DPSM and the calculated acoustic radiation pressure is considered in static fluid analysis in SMAC algorithm as

$$\frac{DU}{Dt} = -\frac{\nabla P}{\rho_w} + \nu \nabla^2 \mathbf{U} + \mathbf{g} + \frac{\boldsymbol{\tau}_R}{(4/3)\rho_w dr}, \quad (3)$$

$$\nabla^2 P = \frac{\rho_w}{\Delta t} \text{div } \mathbf{U}, \quad P = P_{rad} + \sigma \kappa \text{ (on } \Gamma),$$

where P , \mathbf{U} , ρ_w , σ , ν , κ , \mathbf{g} , and Γ are the static pressure, velocity, density, surface tension, dynamic viscosity of the liquid, curvature of the droplet surface, gravity, and set of point on boundary.

[†] yuji.wada@st.seikei.ac.jp

LS-MPS, proposed by Tamai and Koshizuka[9], is higher order differential MPS scheme, is used to calculate the gradient, divergence space differential, and the pressure implicit terms. The viscosity Laplacian is treated in original MPS scheme due to the calculation stability.

Due to the numerical counter torque brought by MPS Laplacian calculation, the rotational coordinate is adopted for the streaming field \mathbf{W} calculation as

$$\omega_L = [I]^{-1} \sum_i^{N_p} (\mathbf{r}_{Li} \times \mathbf{U}_i), \quad (4)$$

$$[I] = \sum_i^{N_p} [(\mathbf{r}_{Li} \cdot \mathbf{r}_{Li})[E] - \mathbf{r}_{Li} \mathbf{r}_{Li}^T],$$

$$\begin{aligned} \mathbf{W} &= \mathbf{U} - \omega_L \times \mathbf{r}_L, \\ \frac{\partial \mathbf{U}}{\partial t} &= \frac{\partial \mathbf{W}}{\partial t} + 2\omega_L \times \mathbf{W} - \omega_L r_L \mathbf{r}_L, \end{aligned} \quad (5)$$

where ω_L , $[I]$, $[E]$, and \mathbf{r}_L are rotational speed and moment of inertia tensor, unit tensor, and position vector from droplet center.

3. Results

Fig. 1 indicates the problem geometry for the ultrasonic droplet levitation and rotation [4, 6]. The upper and lower plane on $z = \pm 3\lambda_1/4$ works as an ultrasonic levitator which is driven on the frequency of $f_1 = 18$ kHz. **Fig. 2** (a) shows the sound field excited by this levitator. The pressure distribution shows third-mode plane standing wave along z -axis and uniform on z -plane.

The plane on $x = \pm \lambda_2/4$ and $y = \pm \lambda_2/4$ in **Fig. 1** works as a pair of acoustic driver with the phase difference of $\pi/2$ between x -planes and y -planes at $f_2 = 1.35$ kHz. **Fig. 2** (b) shows the sound field excited by the driver. Two phase drive create a zero-pressure plane rotating along z -axis, as a result, one nodal point at the coordinate origin is observed in the figure.

Fig. 3 shows the temporal change of the rotational speed with and without the rotational coordinate. The LS-MPS results have complete the calculation as long as 100 ms, whereas the MPS calculation scheme has diverged at 20 ms. While the rotation without rotation has been saturated due to numerical counter torque, the result with rotational coordinate agrees with the experimental result in the error of 25 %.

Fig. 4 (a) (b) shows the streaming field at the time 100 ms calculated with and without the rotational coordinate, where \mathbf{U} and $(\mathbf{W} + \omega_L \times \mathbf{r}_L)$ is plotted in the figure, respectively. As in **Fig. 3**, the outer surface streaming velocity is approximately four times larger with rotational coordinate than the one without rotational coordinate.

4. Conclusion

The streaming on an ultrasonic levitated droplet has been simulated using LS-MPS and DPSM in three dimensional space with rotational coordinate. The trend of the temporal change in rotational speed agrees with the experiment known in Ref. [4].

References

1. L.V. King: Proc. R. Soc. A **147** (1934) 212.
2. W.L. Nyborg: J. Acoust. Soc. Am. **42** (1967) 947.
3. Y. Yamamoto, Y. Abe, A. Fujiwara, K. Hasegawa and K. Aoki: Microgravity Sci. Technol. **20** (2008) 277–280.
4. A. Biswas, E.W. Leung, and E.H. Trinh: J. Acoust. Soc. Am. **90** (1991) 1502.
5. Y. Wada, K. Yuge, R. Nakamura, H. Tanaka, and K. Nakamura: Jpn. J. Appl. Phys., **54**, (2015) 07HE04.
6. Y.Wada, K. Yuge, H. Tanaka, and K. Nakamura: Jpn. J. Appl. Phys., **55** (2016) 07KE06.
7. D. Placko and T. Kundu, Eds, DPSM for Modeling Engineering Problems, 1st edition (Wiley-Interscience) (2007).
8. S. Koshizuka, Y. Oka: Nucl. Sci. Eng. **123** (1996) 421.
9. T. Tamai, and S. Koshizuka: Comput. Part. Mech., **1** (2014) 277.

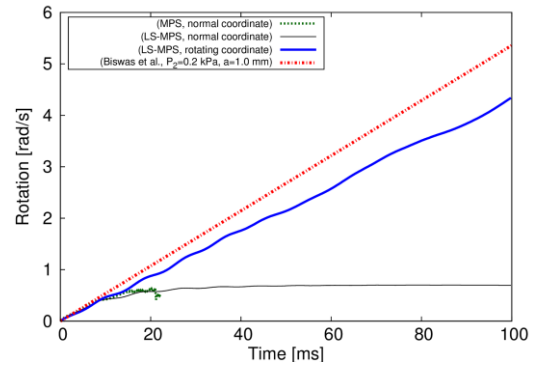


Fig. 3 Temporal change in the rotational speed with and without the rotational coordinate.

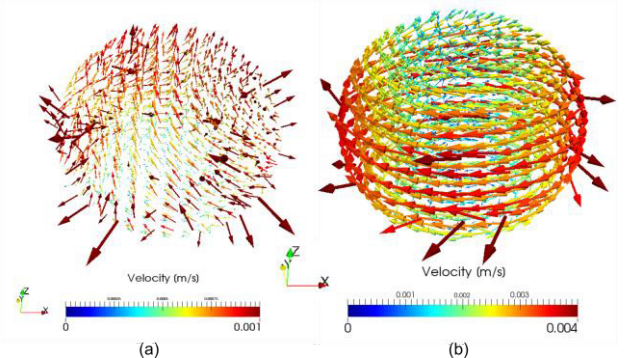


Fig. 4 Streaming distribution (a) without and (b) with the rotational coordinate.